2021 20th International Symposium on Distributed Computing and Applications for Business Engineering and Science (DCABES)

Electrostatic interaction investigations of the Barnase-Barstar complex using molecular dynamics simulation

Yi Fu[1,2]
1. School of Internet of Things Engineering,
Wuxi City College of Vocational Technology
Wuxi, China
2. Wuxi Research Center for Environmental Science & Engineering
fuyi@wxcu.edu.cn

Ji Zhao [1,2]
1. School of Internet of Things Engineering,
Wuxi City College of Vocational Technology
Wuxi, China
2. Wuxi Research Center for Environmental Science & Engineering
ji_zhaowx@163.com

Juan Mei[1,2]
1. School of Internet of Things Engineering,
Wuxi City College of Vocational Technology
Wuxi, China
2. Wuxi Research Center for Environmental Science & Engineering
meijuan_wx@163.com

***Abstract*—Protein-protein interactions can regulate many biological processes. Studying the mechanisms of protein-protein interactions is critical for understanding the biological functions and regulation mechanisms of proteins. The Barnase-Barstar complex is a well-studied target for computational analyses due to its simplicity and small size. Despite extensive studies, it is unclear whether there are differential responses to thermal stress between the Barnase-Barstar complex and the Barnase alone. In this study, molecular dynamics simulations were used to study intermolecular interactions and structural changes of the Barnase-Barstar complex under thermal stress. We performed molecular dynamics simulations under different temperatures for the complex and for Barnase itself. Our simulations suggest that under thermal stress, Barnase is more stable within the Barnase-Barstar complex than the protein itself, and the higher stability is likely attributed to the binding interactions between the two proteins. These results provide a theoretical foundation and an important guidance to understand mechanisms of biological regulation of protein complexes.**

Keywords- Barnase-Barstar complex; salt bridge; electrostatic interaction; molecular dynamics simulation

I. INTRODUCTION

Protein-protein interactions play an important role in biological processes, such as signal transduction, cell regulation, and the immune response [1]. Studies of these interactions are important for understanding biological functions and regulation mechanisms [2-3]. Among protein-protein interactions, binding of different proteins to form protein complex is widespread in all organisms. In *Bacillus amyloliquefaciens*, the Barnase-Barstar complex is a well-studied system, partly due to its simplicity and fast association rates [4]. Barnase is an extracellular ribonuclease with 110 residues from *Bacillus amyloliquefaciens*, and Barstar is a specific intracellular inhibitor of Barnase, produced by the same organism [5]. Barstar can inhibit the intracellular enzymatic activity of Barnase through tight binding to this RNase, thus protect host cells from the damaging effect of Barnase [6].

It is well known that the formation of the Barnase-Barstar complex is mainly driven by electrostatic interactions [7]. Despite the well-recognized role of electrostatics in the formation and stability of Barnase-Barstar complex, the exact effects of changes in the electrostatics during the formation of the system, such as the presence of salt bridges, have not been examined thoroughly. To understand the influence of electrostatics in formation of Barnase-Barstar complex, we aim to analyze the electrostatic interaction behavior of the binding regions of this complex. We have simulated the Barnase-Barstar complex and Barnase alone under varying temperatures. The analysis specifically focuses on the contribution of salt bridges to the binding stability of the complex. Not only is this helpful for us to gain information about the roles of critical residues in the binding domain, but it also allows us to further understand the effects of electrostatic interactions on protein-protein complexes.

II. MATERIALS AND METHODS

The crystal structure of the Barnase-Barstar complex (1BRS) [8] that was obtained from the RSCB protein data bank (http://www.rcsb.org/) was used as a model for our experiment. A single complex (chain A and E) from the crystal structure was used for the complex simulation. As shown in Figure 1, chains A and E from the crystal structure were used for stand-alone protein simulations for Barnase and Barstar respectively.

The protein complex and stand-alone Barnase were subjected to molecular dynamics (MD) simulations using NAMD software [9]. The CHARMM27 force field [10] was used together with the MD simulations. Visual Molecular Dynamics (VMD) [11] was used to generate PSF files for the complex and proteins, in addition to visualization and data analysis. The cubic water boxes which contained TIP3P water molecules [12] were used to solvate the complex and protein. The simulated temperature was set to 300 K, 400 K, 500 K and 600 K, respectively. Through these temperatures, the protein can be observed from the natural to unfolded state. The short-range non-bonded interactions were calculated

2473-3636/21/$31.00 ©2021 IEEE
DOI 10.1109/DCABES52998.2021.00063

using a 12 Å cut-off distance. The long-range electrostatic interactions were calculated by the Particle Mesh Ewald (PME) [13] method. All the bonds involving hydrogen atoms were constrained using the SHAKE method [14]. Firstly, the systems were performed with 10000 steps of steepest descent to finish energy minimization. Then, simulations were performed in NVT ensemble in which the number of particles, N, the volume, V, and the temperature, T, were kept constant. The time for each simulation was set to 10 ns and the time step was set to 2 fs.

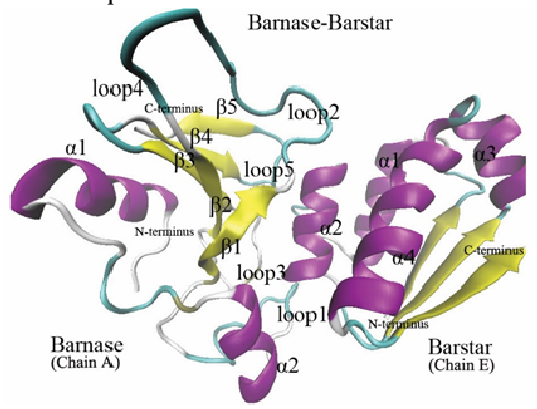

FIG.1. A cartoon representation of the structure of Barnase-Barstar complex

III. EXPERIMENTAL RESULTS AND ANALYSIS

A. The Barnase-Barstar complex confers better structural stability at high temperatures

With molecular dynamics simulation, we probed the stabilities of the Barnase-Barstar complex and the individual protein Barnase. Here, we calculated the Cα root mean square deviation (RMSD) values of the structures in our simulations. The RMSD is a numerical measure to quantify differences between two conformations. It is defined as:

$$RMSD(t_j) = \sqrt{\frac{1}{N_i}\sum_{i=1}^{N_i}(r_i(t_j) - r_0)^2} \qquad (1)$$

where N_i is the number of atoms whose positions are being compared, $r_i(t_j)$ is the position of an atom i at time t_j, and r_0 is the reference value which takes the first time step of the simulation. In general, the RMSD value reflects the mobility of an atom during the molecular dynamics simulation trajectory. A higher residue RMSD value corresponds to higher mobility; conversely, a lower residue RMSD value indicates lower mobility.

The trend of the curves in Fig.2 shows that the systems were equilibrated and suitable to observe the dynamics of the model. In the 300K simulation, the complex and the separate Barnase were very stable throughout the simulation time. Upon inspection of RMSD plots, the average RMSD was found to be 1.64 Å for the Barnase in the complex, and the average RMSD was 1.84 Å for the independent Barnase in the 400 K simulation. In the trajectory run at 500 K, RMSD values of the Barnase in complex clearly increased from the initial conformation, which fluctuated between 0.56 Å and 3.81 Å; the average value of RMSD was 2.43 Å. For Barnase, RMSD values fluctuated between 0.58 Å and 4.57 Å, and the average value was 3.29 Å. When the temperature was set to 600 K, the plots of both the complex and Barnase indicated a clearly increasing trend, with the curves fluctuating more than other lower temperatures. In comparison to the Barnase in complex, with a RMSD value less than 7 Å, the RMSD values of independent Barnase increased significantly up to 12.29 Å. In summary, the RMSD diagrams show the stability of the molecular dynamics simulation trajectories, and they also indicate whether the protein can maintain a natural folding state at a given simulated temperature. When the protein tertiary structure begins to be disrupted, the RMSD value also rises to a higher value.

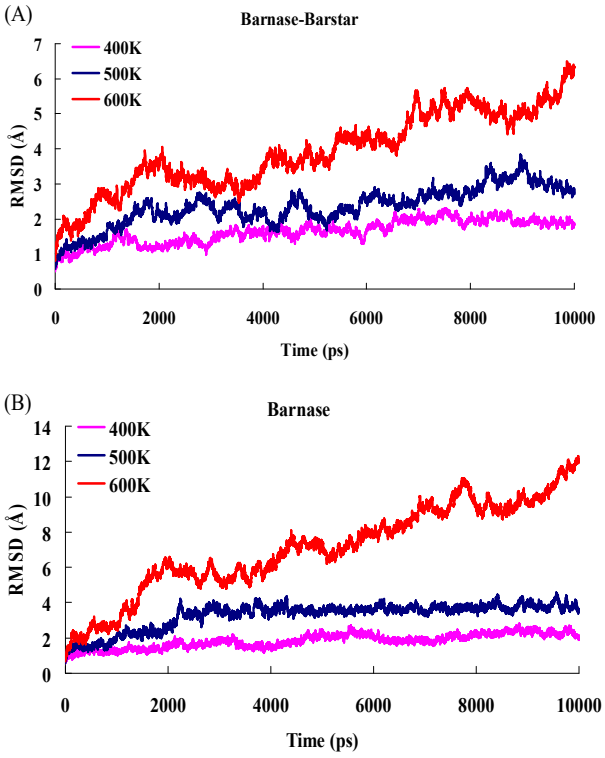

FIG.2 A-B. Root mean square deviation (RMSD) and time evolution plots of the Barnase-Barstar complex and Barnase at different temperatures ((A): Barnase-Barstar; (B): Barnase).

B. Influence of temperature on electrostatic interaction

In the Barnase-Barstar complex, electrostatic complementary regions are important factors that influence the association process and contribute to the stability of the

complex [15]. If charged residues in proteins are located within a certain distance, these residues can form salt bridges. As important contacts in electrostatic interactions, salt bridges have a crucial role in protein stability. To obtain information about the contributions of individual amino acids to complex association, we analyzed the course of salt bridge interactions in the binding regions of the complex. The last 5 ns simulation trajectory was used to analyze the fluctuations of the salt bridges.

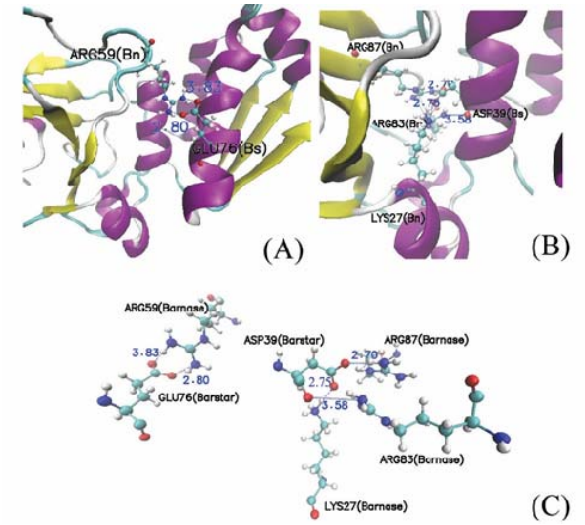

FIG.3 A-C. An overview of the location of salt bridges in the binding domain of the complex. A. The salt bridge between ARG59 and GLU76. B. The salt bridges between LYS27, ARG83, ARG87, and ASP39. C. A close demonstration of the four salt bridges independent of other residues. The blue dotted line represents a salt bridge interaction, and the number next to the dotted line represents the salt bridge distance. Red, oxygen; blue, nitrogen; cyan, carbon; white, hydrogen. (Bn: Barnase; Bs: Barstar)

In the Barnase-Barstar complex, four salt bridges, ARG59-GLU76, ARG83-ASP39, ARG87-ASP39 and LYS27-ASP39, are formed in the binding regions. Fig.3 shows the location of four salt bridges in the binding region. The occupancy of these salt bridges was analyzed in detail to estimate the change of electrostatic interaction. Fig.4 shows the change of salt bridge distance in the last 5 ns of the simulations. In a dynamic simulation at 300 K, these salt bridges were all found to be stable. When the simulation temperature was 400 K, ARG83-ASP39 and ARG87-ASP39 were found to be the most stable among these salt bridges; they were maintained within 4.0 Å distance without any separation. The average distances of ARG83-ASP39 and ARG87-ASP39 were 3.47 Å and 3.51 Å, respectively. In contrast, the salt bridge of ARG59-GLU76 experienced a short separation of approximately 1 ns, but it was stable at approximately 4.0 Å distance the rest of the time. Another salt bridge, LYS27-ASP39, was maintained within a short distance only in the first 1ns of the simulation. Later, the distance of the salt bridge was always more than 5.0 Å. The average distances of salt bridge LYS27-ASP39 were 3.78 Å and 5.56 Å, corresponding to the 300 K and 400 K simulations.

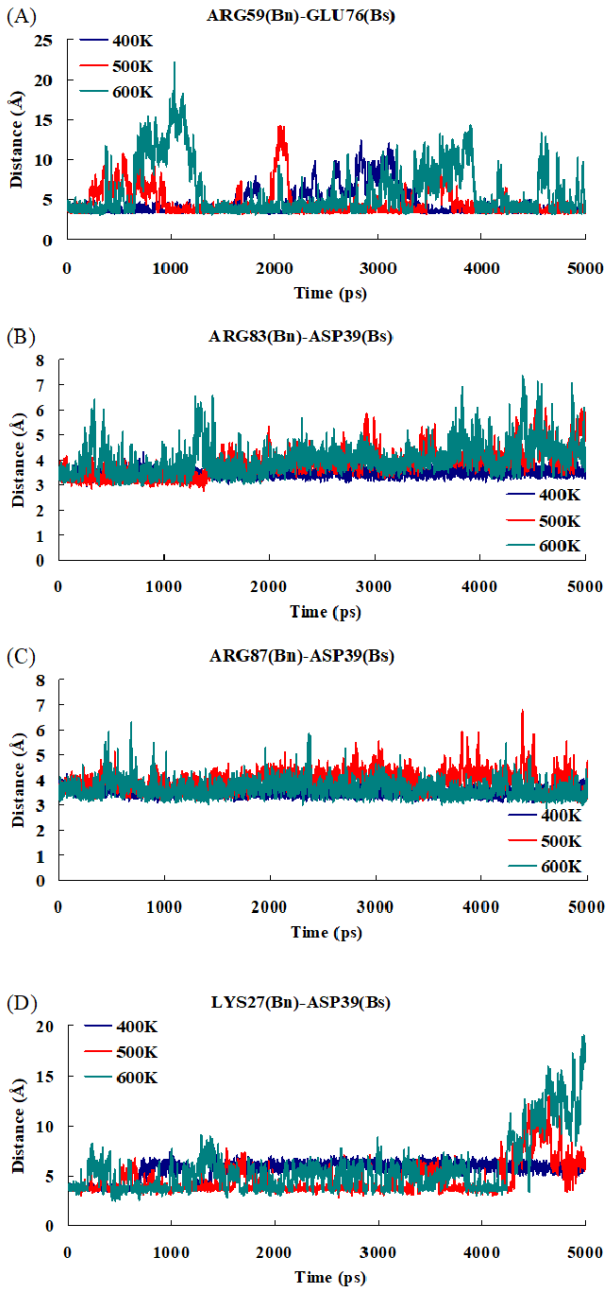

FIG.4 A-D. Plot of salt bridge distance changes as a function of time in the Barnase-Barstar complex binding domain at different temperatures.

Along with the rise of the simulation temperature, the salt bridge distances changed accordingly. In the 500 K

simulation, salt bridges ARG83-ASP39 and ARG87-ASP39 were still stable. Their average distances were 3.82 Å and 3.95 Å, respectively. ARG59-GLU76 was maintained within 4.0 Å for most of the simulation time, with only transient separation of the two residues. At 2061 ps, the distance of the salt bridge was up to 14 Å. However, when the simulation time was 2139 ps, the distance fell back rapidly to 4.08 Å. Salt bridge LYS27-ASP39 was also quite steady except for occasional separation. In general, the salt bridge LYS27-ASP39 in the 500 K simulation was more stable than in the 400 K simulation.

When the temperature increased to 600 K, among the above four salt bridges, ARG87-ASP39 demonstrated the most stable connection. This outcome may be related to the positions of the residues that form the salt bridge; the position of residue ASP39 is located in the α-helix of Barstar, while residue ARG87 is located in the β-sheet of Barnase. Both α-helix and β-sheet are relatively stable in the protein secondary structures. Meanwhile, there is another factor contributing to the stability of the salt bridge. In addition to the ARG87-ASP39 salt bridge, ASP39 can also form interactions with ARG83 and LYS27. In other words, the salt bridge network has a positive role in the relatively high stability of this salt bridge. For salt bridge ARG59-GLU76, ruptures and restorations were observed repeatedly during the whole simulation process.

On the basis of the above results, the distances of four salt bridges were less than 4 Å for most of the time from the 300 K to 500 K simulations. Namely, four salt bridges were well stabilized. The binding regions including these salt bridges were also stable. Thus, these salt bridges contribute to the stability of the complex in terms of binding interactions.

IV. Conclusion

Electrostatic interactions are a significant driving force for biological function. Clarifying the role of electrostatic interactions in protein function and stability is the key for protein engineering and drug design. In this article, we have analyzed electrostatic interactions of the Barnase-Barstar binding region, specifically the stability of salt bridge at different temperatures, using MD simulations. The side-by-side comparison between the complex and protein alone allows us to characterize the main binding features of the complex. Because of the electrostatic interactions in the binding domain, the unfolding temperature of Barnase in complex is higher than that of the independent enzyme. Barnase binds to Barstar residues that are located on a continuous polypeptide fragment; thus the binding interactions could prompt thermal stability of Barnase. Our results also clearly show that salt bridges are of major importance in protein stability at elevated temperature.

This article analyzed the contribution of residues in binding regions to the association of Barnase-Barstar. The results can be served as a reference for designing new thermostable Barnase mutant proteins according to electrostatic interactions. This type of analysis can also be used as an example to understand the role of electrostatic interactions for protein design.

Acknowledgment

This work is supported by the Qing Lan Project of Jiangsu Province (Year 2020 and Year 2019), the Natural Science Foundation of the Jiangsu Higher Education Institutions of China under Grant Nos. 17KJB520039 and Nos. 18KJB520046, the Jiangsu Overseas Visiting Scholar Program for University Prominent Young and Mid-aged Teachers and Presidents.

References

[1] Francois M, Donovan P, Fontaine F. Modulating transcription factor activity: Interfering with protein-protein interaction networks. Seminars in Cell & Developmental Biology, 2020, 99: 12-19.

[2] Goodacre N, Devkota P, Bae E, Wuchty S, Uetz P. Protein-protein interactions of human viruses. Seminars in Cell & Developmental Biology, 2020, 99: 31-39.

[3] Portillo F, Vázquez J, Pajares MA. Protein-protein interactions involving enzymes of the mammalian methionine and homocysteine metabolism. Biochimie, 2020, 173: 33-47.

[4] Kostyukevich Y, Shulga AA, Kononikhin A, et al. CID fragmentation, H/D exchange and supermetallization of Barnase-Barstar complex. Scientific Reports, 2017, 7(1):6176.

[5] Alemany A, Rey-serra B, Frutos S, et al. Mechanical Folding and Unfolding of Protein Barnase at the Single-Molecule Level. Biophysical Journal, 2016, 110(1):63-74.

[6] Neumann J, Gottschalk KE. The Effect of Different Force Applications on the Protein-Protein Complex Barnase-Barstar. Biophysical Journal, 2009, 97(6):1687-1699.

[7] Kieslich CA, Jr RDG, Morikis D. Is the rigid-body assumption reasonable? Insights into the effects of dynamics on the electrostatic analysis of barnase–barstar. Journal of Non-Crystalline Solids, 2011, 357(2):707-716.

[8] Buckle A M, Schreiber G, Fersht A R. Protein-protein recognition: crystal structural analysis of a barnase-barstar complex at 2.0Å resolution. Biochemistry, 1994, 33(30):8878-8889.

[9] Phillips JC, Braun R, Wang W, et al. Scalable molecular dynamics with NAMD. Journal of Computational Chemistry, 2005, 26(16):1781-1802.

[10] MacKerell AD, Bashford D, Bellott M, Dunbrack RL, Evanseck JD, et al. All-atom empirical potential for molecular modeling and dynamics studies of proteins and nucleic acids. The Journal of Physical Chemistry, 1998, 102:3586-3616.

[11] Humphrey W, Dalke A, Schulten K. VMD: visual molecular dynamics. Journal of Molecular Graphics, 1996, 14(1):33-38.

[12] Jorgensen WL, Chandrasekhar J, Madura JD, et al. Comparison of simple potential functions for simulating liquid water. Journal of Chemical Physics, 1998, 79(2):926-935.

[13] Darden T, York D, Pedersen L. Particle mesh Ewald: An N log (N) method for Ewald sums in large systems. Journal of Chemical Physics, 1998, 98(12):10089-10092.

[14] Ryckaert JP, Ciccotti G, Berendsen HJC. Numerical integration of the cartesian equations of motion of a system with constraints: molecular dynamics of n-alkanes. Journal of Computational Physics, 1977, 23(3):327-341.

[15] Mitkevich VA, Schulga AA, Ermolyuk YS, et al. Thermodynamics of denaturation of complexes of barnase and binase with barstar. Biophysical Chemistry, 2003, 105(3):383-390.